

Biomass Fractionation for the Biorefinery: Heteronuclear Multiple Quantum Coherence—Nuclear Magnetic Resonance Investigation of Lignin Isolated from Solvent Fractionation of Switchgrass

Joseph J. Bozell,* C. J. O'Lenick, and Stacy Warwick

Center for Renewable Carbon, Center for Direct Catalytic Conversion of Biomass to Biofuels (C3Bio), University of Tennessee, 2506 Jacob Drive, Knoxville, Tennessee 37996, United States

S Supporting Information

ABSTRACT: Two-dimensional heteronuclear multiple quantum coherence and quantitative ^{13}C nuclear magnetic resonance spectroscopy are used to identify the structural features of lignin isolated from solvent fractionation of switchgrass at several different severities. The spectra are consistent with a progressive deconstruction of the lignin as the fractionation severity increases, with structural units involved in cross-linking and capping of the bulk lignin polymer removed first, followed by increasing levels of acid-catalyzed, solvolytic cleavage of the bulk lignin. The results show that solvent fractionation conditions between about 120 °C and 0.1 M H_2SO_4 and 160 °C and 0.025 M H_2SO_4 are optimal for separating biomass in the biorefinery to give process streams most suitable for biobased fuel and chemical production.

KEYWORDS: HMQC-NMR, solvent fractionation, organosolv, biomass, switchgrass, biorefinery

INTRODUCTION

The goal of the biorefining industry is to convert renewable lignocellulosic feedstocks into fuels and chemicals with a level of efficiency equal to or greater than comparable processes used for nonrenewable raw materials.¹ For chemical production in particular, the first step in this process is the fractionation of the feedstock into its principal components—cellulose, hemicellulose, and lignin—each of which can serve as a primary process stream within the biorefinery.² Understanding the structure of these individual fractionation components is critical for developing downstream conversion processes and tailoring synthetic methodology to the functional group profile resulting from a given separation process. Lignin offers a notable challenge in this regard, because its separation from a biopolymeric matrix almost invariably introduces significant changes to its already complex native structure.³

Our laboratory is investigating switchgrass, a perennial lignocellulosic feedstock under intense current study,^{4,5} as a source of renewable carbon for biobased chemical and fuel production. We have described a solvent-based (organosolv) fractionation process that affords a clean separation of woody biomass.^{6,7} Recently, we have demonstrated that this process can also be used for fractionation of switchgrass into its individual components, including a lignin stream of high purity that we believe will be useful for chemical production (manuscript in preparation). A number of advantages have been reported for organosolv technology in comparison to more conventional pulping processes,⁸ including a more efficient removal of lignin⁹ and improved performance of the cellulose fraction in downstream conversion processes.^{10–12} However, relatively little information is available regarding the structure of the lignin stream obtained from switchgrass after organosolv separation.

One- and two-dimensional (1D and 2D) nuclear magnetic resonance (NMR) spectroscopy has become an invaluable tool

for determining the structural features of lignin. Two-dimensional experiments [heteronuclear multiple quantum coherence (HMQC), heteronuclear single quantum coherence (HSQC), heteronuclear multiple bond correlation (HMBC), and total correlation spectroscopy (TOCSY)] used individually or combined with other 1D and 2D techniques offer significant advantages because of their ability to resolve highly overlapped resonances into a clear roadmap describing the individual substructural units comprising the lignin polymer. A number of reports describe the use of NMR for structural determination of native lignin in grasses and nonwoody plants or herbaceous lignin isolated after biomass pretreatment. Elegant work from Ralph's group relies on HSQC and HMQC experiments for determining the mechanism of lignin biosynthesis in herbaceous feedstocks and changes in lignin structure resulting from up- or down-regulation of key regulatory enzymes.^{13–15} Quantitative 1D ^{13}C and ^{31}P NMR has been used to probe the structure of lignin isolated from autocatalyzed high severity ethanol treatment of *Miscanthus* varieties.¹⁶ HSQC has been used to probe the structure and level of esterification of the lignin C_9 unit side chain in ball-milled native lignins from several herbaceous plants.^{17,18} HSQC has also been used to track the effects of lignin content on the fermentation of sugars derived from transgenic maize stover.¹⁹ One- and two-dimensional HSQC spectra for ball-milled switchgrass lignin isolated before and after dilute acid pretreatment have been reported.^{20,21}

Because of our interest in tailoring synthetic methodology for the structural features present in lignin and the fact that lignin can comprise nearly 20 wt % of herbaceous crops, we have used

Received: May 10, 2011

Accepted: July 27, 2011

Revised: July 26, 2011

Published: July 27, 2011

Table 1. Compositional Analysis of Starting Switchgrass Feedstocks

sample	wt %						
	moisture content	extractives	ash	Klason lignin	total sugars	glucose	xylose
sample 1 (fine grind)	9.2 ± 0.5	10.8 ± 0.3	3.7 ± 0.2	17.9 ± 0.3	61.2 ± 0.8	33.3 ± 1.1	22.8 ± 1.4
sample 2 (fine grind)	6.7 ± 0.1	11.8 ± 1.7	3.6 ± 0.2	17.3 ± 0.6	65.5 ± 0.3	36.7 ± 0.5	23.3 ± 0.4
sample 3 (coarse grind)	7.8 ± 0.1	10.9 ± 1.1	3.7 ± 0.3	17.2 ± 0.2	61.5 ± 0.4	35.3 ± 0.4	21.8 ± 0.6

HMQC to probe the structure of switchgrass lignin samples isolated from a series of solvent fractionation runs carried out under different conditions of temperature and catalyst concentration. To our knowledge, this report is the first 2D NMR study on switchgrass lignin derived from a solvent-based biomass fractionation process.

MATERIALS AND METHODS

Feedstock Analytical Methods. Switchgrass (*Panicum virgatum*) was collected from an established stand of Alamo variety grown in East Tennessee, air-dried, and comminuted in a 1" knife mill to give material approximately 1–2" in length.²² Two treatments of switchgrass were analyzed as follows: fine (~1" in length) and coarsely ground (~2" in length). Analysis for extractives, sugars, and Klason lignin was performed using NREL protocol NREL/TP-510-4268.²³ Compositional analysis for ash was performed using NREL protocol NREL/TP-510-42622.²⁴ Sugar analysis was carried out by high-performance liquid chromatography (HPLC) using a Biorad Aminex HPX-87P column at 85 °C with 10 μ L injections. Table 1 summarizes the results of the analysis.

Solvent Fractionation. Fractionation of switchgrass was carried out as detailed elsewhere.^{6,7} Briefly, approximately 270 g of switchgrass was loaded into a perforated Teflon basket and placed in a Hastelloy C276 flowthrough pressure reactor. The reactor was sealed and placed under vacuum for 30 min. A single-phase mixture of methyl isobutyl ketone (MIBK), ethanol (EtOH), and water (16/34/50 wt %) in the presence of a sulfuric acid catalyst was pulled into the reactor under vacuum and heated to the fractionation temperature. Additional solvent was pumped through the system into a collection tank for 56 min at a rate sufficient to generate approximately 3.5–4.5 L of black liquor. Upon completion of the run, the solvent remaining in the reactor was carefully released into the collection tank. The reactor was cooled and opened, and the Teflon basket containing the undissolved cellulose was removed. Samples for NMR analysis were generated at three temperatures (120, 140, and 160 °C) and H₂SO₄ concentrations (0.025, 0.05, and 0.1M).

Lignin Recovery. Two methods were used to isolate lignin for NMR analysis.

Method 1—Extraction. The black liquor was mixed with 25% v/v deionized water in a separatory funnel, shaken for 1 min, and allowed to stand for 30 min to generate an aqueous and organic phase separated by a thin emulsion. The aqueous phase was drained and collected. The organic phase was filtered through a bed of Celite packed in a Büchner funnel to remove the emulsion. The lignin was isolated from the organic fraction by solvent removal on the rotary evaporator. The resulting lignin residue was triturated by adding diethyl ether, decanting the ether, and then pumping under vacuum overnight. An additional fraction of lignin could be obtained by a second extraction of the aqueous layer with 25% v/v MIBK, followed by solvent removal and trituration. If a second extraction was used, separate NMR spectra were collected for each lignin fraction.

Method 2—Salting Out. The black liquor was mixed with solid NaCl (10 g/100 mL water contained in solvent mixture) in a separatory funnel, shaken, and allowed to stand for 30 min to generate aqueous and organic phases. The layers were separated, and the organic layer was washed once with ~50% v/v water. The layers were separated, and the

organic layer was washed a second time with ~75% v/v water. Lignin was isolated from the organic fraction by solvent removal on the rotary evaporator. The resulting lignin residue was triturated with diethyl ether. After the ether was decanted, the lignin was placed under vacuum. The trituration step was repeated as necessary to give a free-flowing brown powder. Ethanol contained in the combined aqueous fractions was removed on the rotary evaporator to precipitate a second lignin fraction that was isolated by filtration through a double layer of filter paper in a Büchner funnel and dried under vacuum to give a free-flowing brown powder.

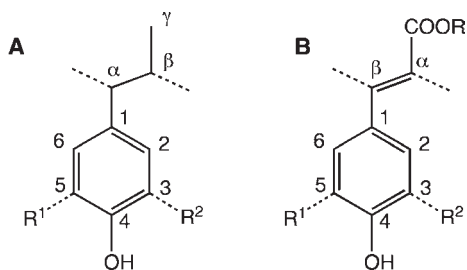
NMR Spectroscopy. Gradient HMQC-NMR measurements were carried out on a Varian 400-MR spectrometer equipped with a broadband probe operating at 399.78 MHz for proton and 100.54 MHz for carbon. A 100–120 mg amount of lignin was dissolved in 750 μ L of DMSO-*d*₆ and filtered into an NMR tube through a small piece of Kimwipe in a Pasteur pipet. Some samples isolated by extraction showed partial solubility, while those isolated by salting out were always fully soluble. The HMQC experiment used 512 increments and 32 scans/increment in the F2 direction, giving a spectrum size of 1024 × 1024. A 90° pulse with a pulse delay of 1.5 s, an acquisition time of 0.13 s, and a one bond C–H coupling constant of 147 Hz were employed. Runs were carried out at 25 °C without spinning and typically required about 16 h. The free induction decays (FIDs) were transformed using Mnova, version 6.2.1, and processed using a *t*₁ noise reduction algorithm, a third-order Bernstein polynomial baseline fit, and Lorentz-to-Gauss apodization using an exponential function of –0.5 Hz and a Gaussian function of 10 Hz in the F₂ direction and an exponential function of –10.0 Hz and a Gaussian function of 90 Hz in the F₁ direction. All spectra were referenced to the residual DMSO signal at 39.5/2.5 ppm. Quantitative ¹³C spectra were measured using inverse gated decoupling and a pulse delay of 11 s. Approximately 18000 scans were taken leading to an experiment time of about 62 h. The FIDs were transformed using Mnova, version 6.2.1, and processed using a Whittaker baseline fit and Lorentz-to-Gauss apodization with an exponential function of 1.5 Hz and a Gaussian function of 1.5 Hz. All spectra were referenced to the residual DMSO signal at 39.5 ppm.

Each NMR sample was prepared identically, but because different fractionation conditions and isolation methodologies lead to different structural profiles, slight differences in peak positions are observed between samples. Table 2 shows average peak locations within two standard deviations observed for five characteristic lignin peaks across 31 different lignin samples. To account for this variance, the peak locations described in this paper are rounded to the nearest ppm for ¹³C and the nearest 0.1 ppm for ¹H.

Nomenclature. Peak designations in this paper use conventional labeling nomenclature employed for lignin C₉ units (Figure 1A). Lignin from grasses also contains significant amounts of conjugated, α,β -unsaturated esters (Figure 1B). However, this commonly employed nomenclature is the reverse of the α,β -designation used for lignin C₉ units (Figure 1A). To avoid confusion, the convention shown in Figure 1A is used exclusively. Substructural units containing the features of Figure 1B are identified as conjugated esters. Individual monolignol units are identified as P (*para*-hydroxyphenyl, to include coumaric acid units), F (ferulic acid and esters), G (guaiacyl), and S (syringyl).

Table 2. Ranges of Peak Locations for Five Characteristic Signals in Switchgrass Lignin (Two Standard Deviations)

C _{2,6} /H _{2,6} in <i>p</i> -coumarate esters	syringyl C _{2,6} /H _{2,6}	C _β /H _β in β-O-4	aromatic OMe	high field alkyls
129.90 ± 0.44/7.52 ± 0.1	103.65 ± 0.22/6.67 ± 0.06	83.29 ± 0.24/4.32 ± 0.04	55.39 ± 0.4/3.74 ± 0.06	13.57 ± 0.24/0.85 ± 0.04

**Figure 1.** (A) Labeling convention for lignin C₉ units used in this paper: P (*para*-hydroxyphenyl), R¹, R² = H; G (guaiacyl), R¹ = H, R² = OCH₃; S (syringyl), R¹, R² = OCH₃. (B) Standard convention for α,β-unsaturated esters.**Table 3. Severities of Fractionations Used in This Study**

temperature (°C)	acid concentration (M)/pH		
	0.025/1.35	0.05/1.0	0.1/0.7
120	0.99	1.34	1.64
140	1.58	1.92	2.22
160	2.16	2.51	2.81

RESULTS AND DISCUSSION

Fractionation of Switchgrass and Lignin Isolation. To approximate operating conditions expected in a commercial biorefinery, the switchgrass was only minimally prepared prior to fractionation. Samples of Alamo switchgrass were air-dried and chopped into 1–2" lengths; however, extractives were not removed nor were plant anatomical fractions (leaves, stems, nodes, and internodes) separated. The process used for fractionation of switchgrass is detailed elsewhere^{6,7} and was carried out by percolating a single phase mixture of MIBK, EtOH, and H₂O (16/34/50 wt %, respectively) through a bed of switchgrass in a pressure reactor at temperatures of 120, 140, and 160 °C and H₂SO₄ concentrations of 0.025, 0.05, and 0.1 M to afford single-phase black liquors containing dissolved lignin, hemicellulose, and extractives. The separations can be classified according to the combined severity constant R_o' , which combines the effects of time, temperature, and acid concentration into a single value.^{25–27} R_o' is defined as:

$$R_o' = \log R_o - \text{pH}$$

where $R_o = (t)^{\exp(\text{Tr}-\text{Tb}/14.75)}$ and t = time of fractionation, Tr = temperature of fractionation, and Tb = baseline temperature, typically 100 °C. Table 3 summarizes the fractionation severities used to generate the samples examined in this paper.

Upon completion of the fractionation, the phase equilibrium of the black liquor is disrupted through the addition of 25% (v/v) water (method 1) or solid NaCl (method 2; 10 g/100 mL water in black liquor), and an organic fraction enriched in lignin was obtained (see Materials and Methods). The yield of lignin from several fractionation runs is summarized in Table 4.

The solubility of the isolated lignin in the NMR solvent (DMSO-*d*₆) varied primarily as a function of the isolation methodology. Extraction, although simple, gave lignin that was only partially soluble from runs carried out at the low (120 °C/0.05 M) and high (160 °C/0.1 M) severity extremes. However, samples between these extremes generally exhibited complete or nearly complete solubility. The total wt % yield of lignin was also lower for samples isolated using extraction, although additional lignin could be obtained by extracting the aqueous phase from the initial black liquor separation with a second portion of MIBK. The yields in Table 4 reflect the total wt % of lignin isolated including any additional extraction stages, and separate NMR spectra were taken for each lignin fraction extracted. In contrast, the more complex salting-out isolation afforded lignins that were always fully soluble in DMSO-*d*₆ regardless of the fractionation conditions. Lignin from salting out partitioned more equally between the aqueous and the organic phases than that isolated by extraction, and thus, separate NMRs for the organic and aqueous lignin samples were collected. Again, the wt % yield in Table 4 represents the combined yield of lignin from both the aqueous and the organic fractions. The final column of Table 4 shows the yield of lignin based on the total amount of Klason lignin determined from compositional analysis of the starting switchgrass feedstock.

Structural Features of Native Herbaceous Lignin. The HMQC spectra provide insight to the lignin deconstruction processes that take place in switchgrass as a function of different solvent fractionation temperatures and acid concentrations. As with most organosolv processes, our fractionation operates under prototypical solvolysis conditions. The switchgrass is treated with excess nucleophilic solvents (EtOH and H₂O) in the presence of an acid catalyst at elevated temperatures, with the added MIBK serving to improve dissolution of lignin and facilitate lignin separation upon workup. Examination of lignin biosynthesis identifies a wide range of sites potentially subject to acid-catalyzed, solvolytic reactions. Lignin's biosynthesis and substructural profile has been widely reviewed,²⁸ but in brief, lignin is constructed from three primary monolignols: *p*-hydroxycinnamyl alcohol, coniferyl alcohol, and sinapyl alcohol (Figure 2). Polymerization is initiated via biochemical hydrogen abstraction from a monolignol to generate intermediate, highly delocalized phenoxy radicals. Lignification results from oxidative coupling of these reactive intermediates to give a complex array of the different substructural units comprising the bulk lignin polymer. In herbaceous biomass, lignin also incorporates significant amounts of *p*-coumaric acid 1 and ferulic acid 2 (Figure 2, inset). Both acids can act as additional monolignols and are incorporated into the polymer during oxidative coupling, primarily at the α-carbon of the lignin side chain.²⁹ Furthermore, ferulic acid undergoes oxidative oligomerization, leading to additional substructural units found in native lignin.³⁰ This family of acids is often esterified to hemicellulose sugars (illustrated in Figure 2 as oligoxylose units), and their coupling to the lignin polymer serves to cross-link lignin with cell wall polysaccharides³¹ at the periphery of the bulk polymer.¹⁹ *para*-Coumaric acid is also incorporated through ester linkages at the γ-position of syringyl

Table 4. Summary of Individual Switchgrass Fractionation Runs and Lignin Yields

run no.	H ₂ SO ₄ (M)	temperature (°C)	lignin yield (wt %) ^a	separation method	solubility ^d	yield based on lignin in feedstock (%)
1	0.05	120	5.42	1	P	31.89
2	0.05	120	2.02	1	P	11.89
3	0.1	120	14.55	2	F	85.60
4	0.1	120	16.48	2	F	96.96
5	0.025	140	11.50	1 ^b	F	67.64
6	0.05	140	4.57	1	P	26.89
7	0.05	140	6.95	1	P	40.88
8	0.05	140	ND ^b	2	F	ND ^b
9	0.1	140	13.01	2	F	76.51
10	0.1	140	10.90	2	F	64.10
11	0.025	160	14.08	1 ^c	F	82.81
12	0.025	160	16.40	1 ^c	P	96.47
13	0.05	160	11.46	1 ^c	F	67.40
14	0.05	160	15.02	1 ^c	F	88.38
15	0.1	160	8.46	1 ^c	e	49.79
16	0.1	160	13.49	1 ^c	e	79.35
17	0.1	160	12.55	2	F	73.83

^a Total yield of lignin after all extractions or isolated from all fractions. ^b Lignin collected from a multirun campaign—yields from each individual run were comparable to other runs isolated using method 2. ^c Additional lignin was obtained in a second extraction of the aqueous phase. ^d P = partial, and F = full. ^e The first fraction collected was partially soluble, and the second was fully soluble.

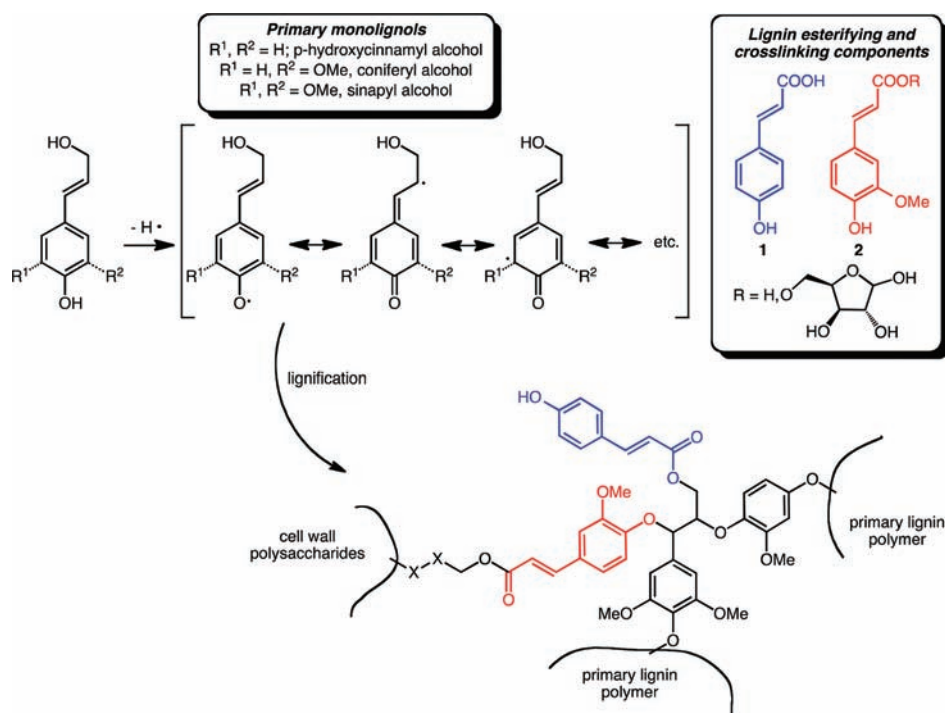


Figure 2. Schematic representation of the lignification process and the primary structural features present in herbaceous lignin (X = xylose).

side chains where it is implicated in polymerization of syringyl units late in lignin formation.³² From a chemical standpoint, any of these resulting ether and ester linkages presents a suitable target for acid promoted solvolytic reaction.

HMQC-NMR Results and Mechanistic Implications. Figure 3A shows the HMQC spectrum for a fully soluble lignin sample obtained from the organic fraction of a separation carried out at 140 °C/0.05 M. For analysis, the spectra are divided into four partially overlapping

regions: a carbonyl region between 200 and 175/10.0–9.0 ppm (¹³C/¹H), an aromatic region between 160 and 90/8.0–6.0 ppm, a side chain region between 110 and 50/6.0–2.5 ppm, and an alkyl region between 50 and 10/3.0–0.5 ppm. Figures 3B–D show subspectra of Figure 3A for the aromatic, side chain, and alkyl regions. Table 5 summarizes the observed HMQC signals and their corresponding peak assignments for all spectra collected in this study, based on correlation with model compounds, peak assignments from

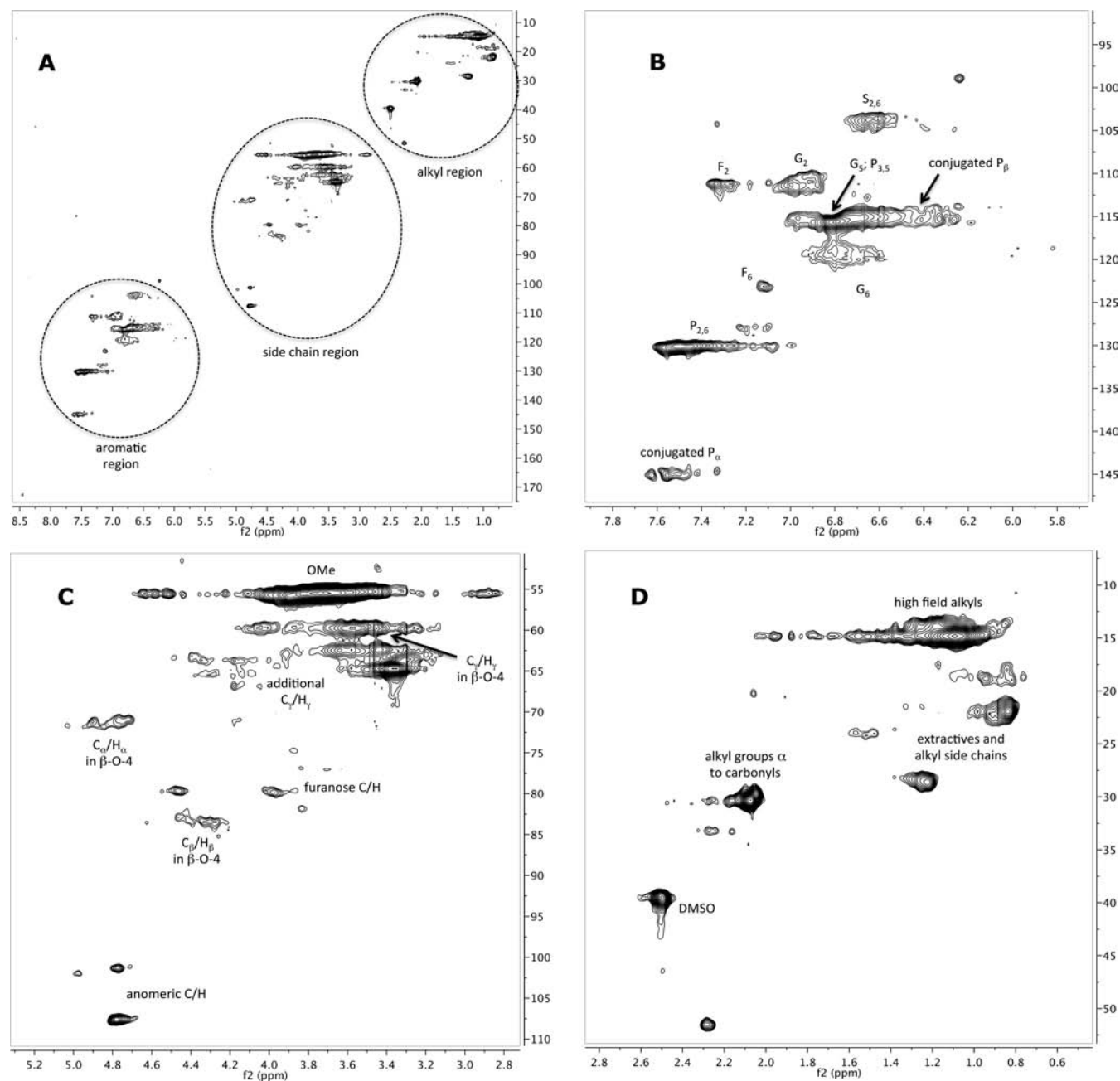


Figure 3. Typical HMQC spectra of switchgrass lignin from solvent fractionation. A, full spectrum; B, aromatic region subspectrum; C, side chain region subspectrum; and D, alkyl region subspectrum.

related lignin NMR studies, available databases, or commercial software.^{15,17,33–36} Accordingly, not all signals listed in Table 5 appear in Figure 3, but all spectra contributing to Table 5 are included as Supporting Information.

Overall, the NMR analysis reveals a relatively wide range of conditions that lead to roughly similar HMQC spectra. Across this range, a corresponding increase in the yield of lignin and in the number and diversity of signals for typical lignin substructures is observed by HMQC. The spectra further reveal signals consistent with acid-catalyzed nucleophilic and solvolytic reaction of the lignin with the fractionation solvent, for example, the gradual disappearance of β -O-4 linkages at increasing fractionation severity or the appearance of alkoxy substitution

at the α -position of the lignin C₉ side chain. Figure 4 summarizes the major categories of structures identified from the HMQC measurements detailed in the following sections, an approximate indication of conditions resulting in their initial appearance, and the point when the structures are no longer observed.

Carbonyl Region. Peaks corresponding to aldehyde functional groups are irregularly observed as weak signals at 191/9.8, beginning at 120 °C/0.1 M. This region also periodically exhibits an unidentified peak at 178/9.6 in several samples.

Aromatic Region. At the mildest fractionation conditions (120 °C/0.05 M), HMQC spectra suggest that the dominant process is release of units involved in cross-linking of lignin to cell

Table 5. Correlation Chart for Signals Observed in Switchgrass Lignin from Solvent Fractionation

typical signal location ($^{13}\text{C}/^1\text{H}$)	assignment
	carbonyl region
195.81/9.94; 188.98/9.55	aldehyde C/H
177.84/9.55	unidentified
	aromatic region
155.36/8.30; 155.84/8.08; 148.55/8.08	$\text{C}_{2,6}/\text{H}_{2,6}$ in P units with α -carbonyl
144.51/7.60; 144.48/7.53; 143.87/7.56	$\text{C}_\alpha/\text{H}_\alpha$ in conjugated esters
131.17/7.66	$\text{C}_{2,6}/\text{H}_{2,6}$ in P groups with esterified 4-OH
129.05/5.30; 126.62/5.12; 98.95/6.22	unidentified
129.59/7.46	$\text{C}_{2,6}/\text{H}_{2,6}$ in P units
128.25/7.67	$\text{C}_{2,6}/\text{H}_{2,6}$ in esterified at C-4
127.77/7.21; 129.82/7.25	$\text{C}_{2,6}/\text{H}_{2,6}$ in P with α -OH or OR
124.14/7.48; 122.59/7.52	G C_6/H_6 with carbonyl at α -position of side chain
122.72/7.09	F C_6/H_6
118.18/6.73	guaiacyl C_6/H_6
115.02/6.94; 115.24/6.78	G C_5/H_5 , P $\text{C}_{3,5}/\text{H}_{3,5}$
114.86/6.41; 114.64/6.31	$\text{C}_\beta/\text{H}_\beta$ in ferulates
111.91/6.68	C_5 in G units etherified at C-4; C_2 or C_6 in phenylcoumarans
110.74/7.26	C_2/H_2 in esterified ferulates or free ferulic acids
110.63/6.90	G C_2/H_2
109.49/6.61	4-O-5
107.63/4.78	alkyl glycoside anomeric peak
106.79/7.22	S $\text{C}_{2,6}/\text{H}_{2,6}$ with carbonyl at α -position of side chain
104.35/6.90	unidentified
103.37/6.65	S $\text{C}_{2,6}/\text{H}_{2,6}$
	side chain region
101.88/4.99; 101.38/4.76; 98.70/4.64; 98.48/4.60; 92.18/4.88	anomeric position in furanose rings
98.84/6.25	unidentified
86.89/5.47	$\text{C}_\alpha/\text{H}_\alpha$ in phenylcoumaran
83.34/4.31	$\text{C}_\beta/\text{H}_\beta$ in β -O-4
82.16/3.77; 80.02/3.96; 77.01/3.71; 76.79/3.82; 74.75/3.85	furanose OH
79.50/4.44	lignin-carbohydrate linkages
72.35/4.73	$\text{C}_\alpha/\text{H}_\alpha$ in β -O-4
72.83/3.34; 71.66/3.20; 69.34/3.49	pyranose OH
66.99/4.11	γ -ethers
63.81/4.19; 63.66/4.34	$\text{C}_\gamma/\text{H}_\gamma$ with esterified γ -OH
62.53/3.38	aryl glycerol
62.31/3.87	$\text{C}_\gamma/\text{H}_\gamma$ in phenylcoumaran
62.48/3.63; 61.86/3.39	various $\text{C}_\gamma/\text{H}_\gamma$ in side chain
59.54/4.04	$\text{C}_\gamma/\text{H}_\gamma$ in P units
59.76/3.61; 59.90/3.31	$\text{C}_\gamma/\text{H}_\gamma$ in β -O-4
55.72/4.51	unidentified
55.44/3.73	methoxy
55.43/2.94; 55.3/2.83	$\text{C}_\beta/\text{H}_\beta$ in β -1
52.85/3.47	$\text{C}_\beta/\text{H}_\beta$ in phenylcoumaran
	alkyl region
51.57/2.29; 22.05/0.81	solvent
33.27/2.17	benzylic CH_2
29.68/2.04; 29.44/2.07	alkyl groups α to a carbonyl and/or solvent
28.49/1.24; 26.29/1.99; 24.10/1.48	CH signals in extractives and aliphatic lignin chains
14.90/1.07; 13.54/0.84; 10.53/0.86	high field alkyls

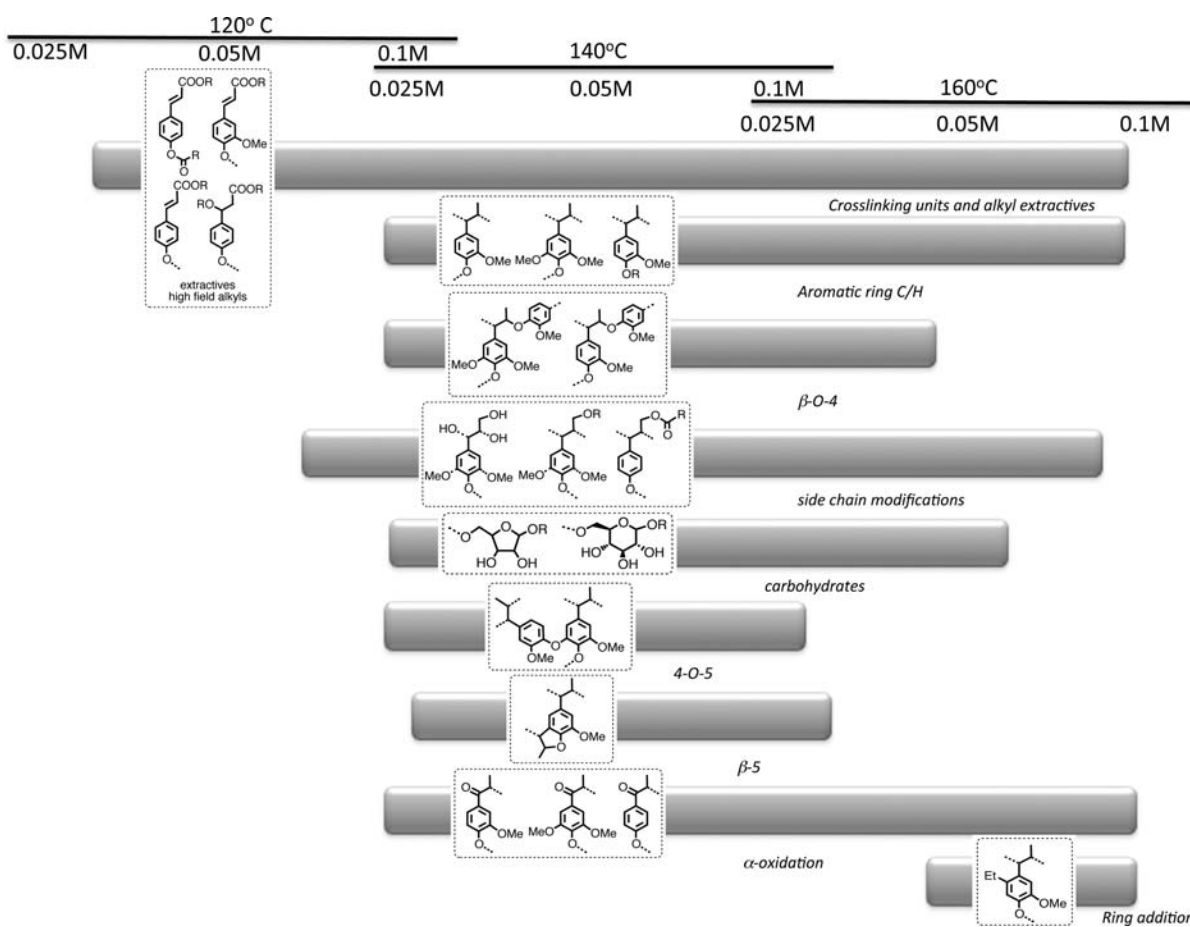


Figure 4. Summary of structures observed in HMQC evaluation of lignin samples from switchgrass as a function of fractionation conditions.

wall polysaccharides. Signals for $C_{2,6}/H_{2,6}$ and $C_{3,5}/H_{3,5}$ positions in P units appear at 130/7.5 and 115/6.8. P units appear particularly reactive to acid-catalyzed solvolysis as these peaks are observed, albeit weakly, even for lignin samples isolated at 120 °C/0.025 M. The $C_{2,6}/H_{2,6}$ signal in P units is sometimes flanked by signals at 131/7.7 and 128/7.7, consistent with $C_{2,6}/H_{2,6}$ in P groups esterified at the 4-position. These flanking peaks diminish in intensity as fractionation severity is increased and disappear completely at 160 °C/0.025 M. The $C_{3,5}/H_{3,5}$ signal for P units overlaps with the corresponding C_5/H_5 signal in G units, but P units appear to dominate fractionations carried out at 120 °C/0.05 M, as the G unit C_2/H_2 and C_6/H_6 signals at 111/6.9 and 118/6.7 are weak. F units are also observed at mild conditions, with C_6/H_6 and C_2/H_2 appearing at 123/7.1 and 111/7.3, respectively. The presence of F and P units are supported by their side chain signals for C_α/H_α at 145–144/7.6–7.5 and C_β/H_β between 115/6.4–6.3. Signals for P and F units are persistent and continue to appear under all fractionation conditions.

Beginning at about 120 °C/0.1 M or 140 °C/0.025 M (approximately equal severities, Table 3), more extensive lignin disassembly is observed, consistent with continued cleavage of crosslinking units and initial solvolysis of the bulk lignin polymer. Well-established, characteristic peaks for aromatic ring C/H positions in G and S units appear (Table 4) and persist across subsequent runs at increasing severity. Of particular interest are signals consistent with introduction of oxygen at the α -position of the side chain in each of the primary monolignols. Signals

at 149/8.1, 124–123/7.5, and 107/7.27 are consistent with the C_2/H_2 or $C_{2,6}/H_{2,6}$ positions of P, G, and S units, respectively, that possess a carbonyl group at the α -position of the side chain. These signals first appear for G units at 120 °C/0.1 M, for S units at 140 °C/0.025 M, and for P units at 140 °C/0.1 M. The relative strength of these signals varies as a function of isolation method at lower temperatures and acid conditions but increases with increasing fractionation severity. Alternatively, side chain oxygenation occurs through the introduction of OH or OR groups at the α -position of the lignin side chain as indicated by signals at 130/7.3 and 128/7.2 beginning at 120 °C/0.1 M. These signals persist throughout fractionations carried out at increasing severity. A well-resolved signal appears at 109/6.6 beginning at 120 °C/0.1 M and persists through most subsequent fractionations. The location of this signal is consistent with the C_2/H_2 position of 4-O-5 structures bearing a side chain oxidized at the α -position³⁶ but requires more extensive investigation to verify this assignment.

α -Oxygenation results from solvolysis of substructural units within the bulk lignin polymer and is a likely primary path for switchgrass fractionation (Figure 5). In the presence of acid and aqueous EtOH, α -O-4 and β -O-4 units are cleaved to give either intermediate enol ethers (3) or quinone methide structures (5). Hydrolysis of 3 affords aryl ketone 4. Reaction of 5 with EtOH or H₂O leads to introduction of hydroxy or alkoxy groups at the α -position of the lignin side chain. Alternatively, conjugated P or F units (6) may undergo acid-catalyzed Michael type additions

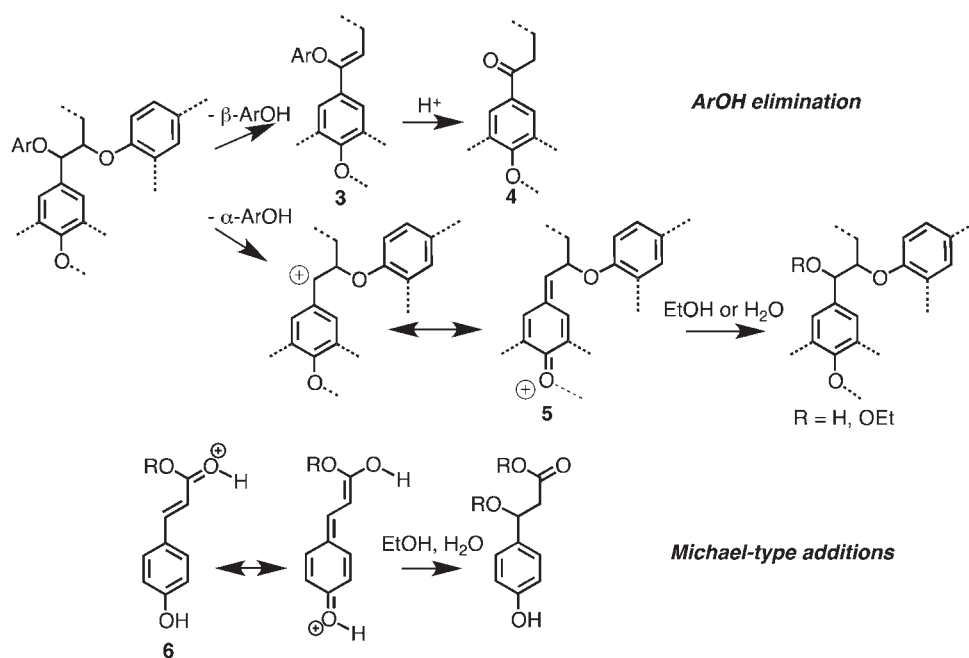


Figure 5. Solvolytic mechanisms for introduction of oxygen into lignin side chains.

of solvent, also leading to hydroxylation or etherification at the α -position.^{37,38} At high severity (160 °C/0.05 M and higher), signals for the C_6/H_6 position in G units weaken in comparison to the C_5/H_5 signals, suggesting that electrophilic reactions at the aromatic ring may be occurring. Condensation with other aromatic units has been suggested as a possible reaction in organosolv treatments of biomass carried out under conditions more severe than those reported here.³⁹ Alternatively, the reaction conditions are conducive to the electrophilic introduction of an ethyl group (from EtOH). Further work is underway to verify the presence of such structures.

Side Chain Region. Under mild conditions (120 °C/0.05 M), the side chain region is initially populated only by the characteristic aromatic ring OCH_3 at 55/3.8 and a few signals corresponding to the side chain C_γ/H_γ structures. The C_γ/H_γ signal in P units is observed at 59/4.0 at the mildest conditions and persists through most subsequent separations. Markedly greater complexity is observed in this region as the severity of the fractionation increases. C_α/H_α signals for phenylcoumaran (β -5) structures first appear at 120 °C/0.1 M and are supported by corresponding C_γ/H_γ and C_β/H_β at 62/3.9 and 53/3.5, respectively. These structures are observed in fractionations carried out up to 140 °C/0.1 M but disappear by 160 °C/0.025 M. The C_α/H_α signal frequently has two components, suggesting that related structures are present, consistent with the ability of phenylcoumaran structures derived from F unit oligomerization to be incorporated into lignin.³⁰ β -O-4 structures are first observed at 120 °C/0.1 M and are identified by the C_β/H_β signal at 83/4.3. Signals for β -O-4 structures in S units at 86/4.1 are normally weak or absent. We attribute this to high levels of acylation at the γ -OH group of the S unit side chains, which moves the C_β/H_β signal to the location observed.⁴⁰ The corresponding C_α/H_α are observed at 71/4.8 and 71/4.9. C_γ/H_γ signals are seen at 60/3.6–3.3. β -O-4 structures reach a maximum in runs carried out between 140 °C/0.05–0.1 M and then decrease. The signals are weak or absent in runs carried out at 160 °C. Cleavage of β -O-4

bonds takes place via the mechanism shown in Figure 5, and the gradual increase and prominence of signals corresponding to α -oxygenation of the lignin side chain are consistent with this process.

A wide range of different signals for the C_γ/H_γ position of the side chain are observed as a complex set of signals between 67 and 59/4.0–3.3. This observation is not surprising as each position present in the side chain of the monolignols is subject to solvolytic cleavage and subsequent reaction. Prototypical signals for this position of the side chain are observed beginning at 120 °C/0.1 M and are generally present thereafter. Different substitution patterns on the side chain are observed. Diffuse signals at 64/4.2 and 64/4.3 appear frequently starting at 120 °C/0.1 M H_2SO_4 and are consistent with esterified γ -OH groups on the side chain. The formation of γ -ethers as an alternate substitution is suggested by a signal at 67/4.1, prominent in many samples. The presence of aryl glycerols is suggested by the signal at 63/3.4.

Several fractionations exhibit a variety of peaks that we assign to carbohydrates based on comparison to reported 2D NMR analysis of other lignins and predictions using commercial software (Figure 6). Carbohydrate structures first appear at 120 °C/0.1 M, with the greatest diversity and number of signals appearing at 140 °C/0.05 M. Subsequent runs at higher severity show a declining number of peaks until they have largely disappeared at 160 °C/0.1 M. The large number of peaks in these regions makes assignment to specific structural features difficult but show increasing amounts of solvolysis and release of both pentose and hexose structures likely involved in cross-linking of lignin to the switchgrass cell wall.

Signals for the anomeric position of carbohydrate-containing structures appear at 110–90/6.2–4.5 ppm. Signals observed in the range of 84–74/4.0–3.6 ppm are primarily associated with furanose sugars, while those between 78 and 68/3.5–2.9 ppm are primarily associated with pyranose sugars.^{17,41,42} The furanose signals appear more frequently than those for the

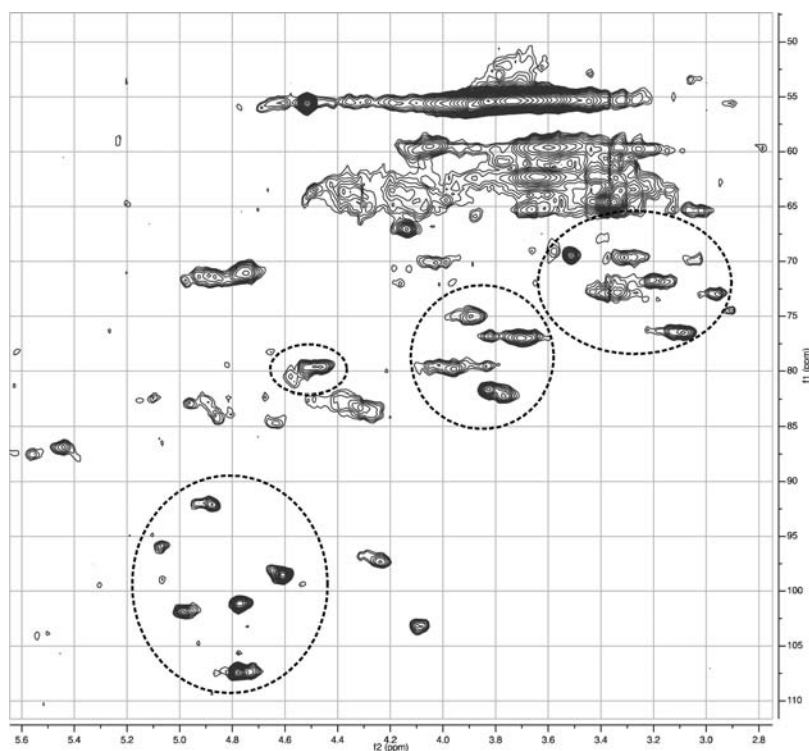


Figure 6. Carbohydrate signals observed in HMQC spectra at 140 °C/0.025 M H₂SO₄.

pyranose sugars; however, this may be a function of differences in the lignin isolation procedure.

Alkyl Region. Lignin samples isolated at low severity (120 °C/0.05 M) exhibit a significant number of peaks in the alkyl region, while the other spectral regions are more sparsely populated. These peaks are maintained through all subsequent fractionations. High field peaks observed at 15–14/1.1–0.9 are consistent with aliphatic methyl and methylene groups in the lignin propyl side chain, and several spectra reveal the presence of a series of well-resolved methyl groups at 21–11/0.9 ppm. Specific signals at 19/0.9–0.8 have been assigned to ethoxy groups, consistent with other peaks present in aromatic region resulting from EtOH addition to benzylic position.³⁹ Signals at 24/1.5 and 29/1.2 are associated with extractives present in the starting feedstock and appear at most fractionation conditions. Such peaks are expected, as the starting feedstock was not treated to remove extractable material prior to fractionation. Peaks appearing between 33 and 24/2.3–1.9 are likely CH₂ groups α to carbonyl groups, consistent with α -O-4 and β -O-4 cleavages, and the production of Hibbert-like ketones.⁴³ These signals appear at higher severities and are consistent with the corresponding peaks for α -side chain oxidation present in the aromatic region of the spectrum.

Quantitative ¹³C Measurements. Quantitative ¹³C was used to measure the relative population of several peak clusters in fully soluble switchgrass lignin samples isolated by salting out. The solvent fractionated material was then normalized to values recently reported for ball-milled switchgrass lignin²⁰ to determine which structural units were affected during the fractionation process (Table 6). The cluster at 162–140 ppm (oxygenated aromatic carbons, C _{α} in F and P units) was used as the baseline.

The greatest changes occur for those peak clusters most sensitive to the solvolytic conditions of the fractionation. In

all lignin samples from the organic fraction, fractionation reduces the relative amount of material in the 123–102.5 ppm cluster, assigned to aromatic C–H groups and the C _{β} in F and P units. However, this relative amount changes little as the severity of the fractionation increases. Because these structures are not likely to undergo solvolytic reactions during the fractionation, the differences may be due to the composition of the starting switchgrass feedstock. The ball-milled material was reported to have 22.7% lignin, while the switchgrass in this study contained only 17% lignin. Similarly, the relative amount of material in the 65–58 ppm cluster, assigned to the C _{γ} in β -O-4 and esterified P units, is slightly elevated but remains relatively constant at different severities. In contrast, the relative amount of material in the 88–77 ppm cluster, assigned to the C _{β} in β -O-4 and the C _{α} in β -5, starts at levels comparable to ball-milled material but ultimately drops to a much lower level at high severities, consistent with the higher reactivity of these units under solvolysis conditions. The 77–65 ppm cluster, assigned to C _{α} in β -O-4 and xylan ring C–OH, begins at a much lower relative level than in ball-milled lignin. As our process is designed to separate the cellulose and hemicellulose from the lignin, this difference probably reflects a higher amount of carbohydrate retained in the ball-milled material. HSQC measurements of ball-milled switchgrass lignin confirm this significantly higher level of carbohydrate, which is also observed even after a dilute acid treatment.²¹ These results support our earlier observations that solvent treatment is significantly more effective at removing carbohydrates from the lignin fraction.⁷ Additional experiments are underway to more completely integrate these results with mechanisms of lignin deconstruction and release from the cell wall.

Impact of Lignin Isolation Methods on Spectra. Both lignin isolation methods used in this study generate multiple samples for NMR analysis, but differences in the HMQC spectra for the

Table 6. Integration of Peak Clusters in Several Lignin Samples Isolated by Salting Out

run conditions	NMR region (ppm)				
	162–140 ^a	123–102.5 ^b	88–77 ^c	77–65 ^d	65–58 ^c
120 °C/0.1 M (organic fraction)	100.00	89.80	30.61	1.02	53.06
140 °C/0.1 M (organic fraction)	100.00	93.94	17.17	1.01	31.31
160 °C/0.1 M (organic fraction)	100.00	87.63	4.12	3.09	49.48
ball-milled switchgrass lignin	100.00	110.53	36.84	50.72	43.54

^a Assignment: ²⁰Oxygenated aromatics, C_α in F and P units. ^b Assignment: ²⁰Aromatic methines, C_β in F and P units. ^c Assignment: ²⁰C_β in β-O-4. ^d Assignment: ²⁰C_α in β-O-4, pentoses. ^e Assignment: ²⁰C_γ in β-O-4, F and P esters.

two methods are generally slight, that is, a single spectrum from extracted lignin is normally a composite of the spectra obtained for the aqueous and organic samples obtained by salting out, even for samples that display reduced solubility in DMSO-*d*₆. However, differences are observed for multiple spectra obtained for a given separation method. For example, lignin isolated at low to intermediate severity exhibits peaks for P units at 130/7.5, periodically accompanied by peaks for esterified P units at 131/7.7 and 128/7.7. These flanking peaks appear only with the aqueous lignin for samples isolated by salting out. Furthermore, carbohydrate-containing fragments in samples isolated by salting out are more prominent in the organic lignin than the aqueous, suggesting that the addition of salt may be effective in forcing marginally soluble components into the organic fraction. When extraction is used to isolate lignin from high severity runs, the initially extracted material exhibits an HMQC spectrum with relatively few features. However, material isolated after a second extraction step generally exhibits signals prototypical for normal lignin samples. We currently believe that this observation suggests a greater amount of lignin structural degradation occurs at higher severities and that a second extraction is needed to remove fragments of lower molecular weight from the aqueous component of the black liquor. These differences indicate that the separation methodology may be adapted to promote a more selective separation of the lignin; however, these results are preliminary and still under development.

HMQC analysis of lignin isolated from solvent fractionation at different temperatures and acid concentrations gives insight as to the mechanism of lignin deconstruction and the functional group profile that may be exploited in downstream conversion to chemicals and fuels. The spectra are consistent with a progressive deconstruction of the lignin, in which structural units involved in cross-linking and capping of the bulk lignin polymer are removed first, followed by increasing levels of acid-catalyzed, solvolytic cleavage of the bulk lignin. The results continue to confirm that in our system, fractionation conditions between about 120 °C/0.1 M and 160 °C/0.025 M offer the best opportunity for use in the biorefinery, and the ability to generate separate process streams most suitable for biobased fuel and chemical production. If lower severities are employed, poor lignin removal is observed. Operation at higher severities gives increased lignin fragmentation but a possibly overall poorer separation of the lignin and carbohydrate components, as well as a severe discoloration of the isolated cellulose. Work is continuing to develop conditions for more selective fractionation and isolation of potentially valuable low molecular weight lignin components and to quantify differences in composition of lignin obtained from different workup methods.

■ ASSOCIATED CONTENT

Supporting Information. HMQC spectra for all samples described in the manuscript. This material is available free of charge via the Internet at <http://pubs.acs.org>.

■ AUTHOR INFORMATION

Corresponding Author

*Tel: 865-974-5991. Fax: 865-946-2085. E-mail: jbozell@utk.edu.

Funding Sources

This work was funded by the U.S. Department of Transportation through the Southeastern Regional Sun Grant program.

■ ACKNOWLEDGMENT

Lindsey Kline carried out the compositional analysis on the starting feedstock. We thank Professor John Ralph and Dr. Hoon Kim (University of Wisconsin) for discussions regarding NMR experimental design and interpretation and Professor Al Womac (University of Tennessee) for the switchgrass used in this study.

■ REFERENCES

- Bozell, J. J.; Petersen, G. R. Technology development for the production of biobased products from biorefinery carbohydrates—the U.S. Department of Energy's "Top 10" revisited. *Green Chem.* **2010**, *12*, 539–554.
- Bozell, J. J. An evolution from pretreatment to fractionation will enable successful development of the integrated biorefinery. *BioResources* **2010**, *5*, 1326–1327.
- Mosier, N.; Wyman, C.; Dale, B.; Elander, R.; Lee, Y. Y.; Holtzapfel, M.; Ladisch, M. Features of promising technologies for pretreatment of lignocellulosic biomass. *Bioresour. Technol.* **2005**, *96*, 673–686.
- Keshwani, D. R.; Cheng, J. J. Switchgrass for bioethanol and other value-added applications: A review. *Bioresour. Technol.* **2009**, *100*, 1515–1523.
- Sanderson, M. A.; Reed, R. L.; McLaughlin, S. B.; Wullschlegel, S. D.; Conger, B. V.; Parrish, D. J.; Wolf, D. D.; Taliaferro, C.; Hopkins, A. A.; Ocumpaugh, W. R.; Hussey, M. A.; Read, J. C.; Tischler, C. R. Switchgrass as a sustainable bioenergy crop. *Bioresour. Technol.* **1996**, *56*, 83–93.
- Black, S. K.; Hames, B. R.; Myers, M. D. U.S. Patent 5,730,837, 1998.
- Bozell, J. J.; Black, S. K.; Myers, M.; Cahill, D.; Miller, W. P.; Park, S. *Biomass Bioenergy* **2011**, in press (DOI:10.1016/j.biombioe.2011.07.006).
- Pye, E. K.; Lora, J. H. The Alcell process—A proven alternative to kraft pulping. *Tappi J.* **1991**, *74*, 113–118.

- (9) Oliet, M.; Garcia, J.; Rodriguez, F.; Gilarranz, M. A. Solvent effects in autocatalyzed alcohol-water pulping: Comparative study between ethanol and methanol as delignifying agents. *Chem. Eng. J.* **2002**, *87*, 157–162.
- (10) Shatalov, A. A.; Pereira, H. Polysaccharide degradation during ozone-based TCF bleaching of non-wood organosolv pulps. *Carbohydr. Polym.* **2007**, *67*, 275–281.
- (11) Sixta, H.; Harms, H.; Dapia, S.; Parajo, J. C.; Puls, J.; Saake, B.; Fink, H. P.; Roder, T. Evaluation of new organosolv dissolving pulps. Part I: Preparation, analytical characterization and viscose processability. *Cellulose* **2004**, *11*, 73–83.
- (12) Ruzene, D. S.; Goncalves, A. R.; Teixeira, J. A.; De Amorim, M. T. P. Carboxymethyl cellulose obtained by ethanol/water organosolv process under acid conditions. *Appl. Biochem. Biotechnol.* **2007**, *137*, 573–582.
- (13) Ralph, J.; Akiyama, T.; Kim, H.; Lu, F. C.; Schatz, P. F.; Marita, J. M.; Ralph, S. A.; Reddy, M. S. S.; Chen, F.; Dixon, R. A. Effects of coumarate 3-hydroxylase down-regulation on lignin structure. *J. Biol. Chem.* **2006**, *281*, 8843–8853.
- (14) Ralph, J.; Hatfield, R. D.; Quideau, S.; Helm, R. F.; Grabber, J. H.; Jung, H. J. G. Pathway of *p*-coumaric acid incorporation into maize lignin as revealed by NMR. *J. Am. Chem. Soc.* **1994**, *116*, 9448–9456.
- (15) Yelle, D. J.; Ralph, J.; Frihart, C. R. Characterization of nonderivatized plant cell walls using high-resolution solution-state NMR spectroscopy. *Magn. Reson. Chem.* **2008**, *46*, 508–517.
- (16) El Hage, R.; Brosse, N.; Chruscziel, L.; Sanchez, C.; Sannigrahi, P.; Ragauskas, A. Characterization of milled wood lignin and ethanol organosolv lignin from *Miscanthus*. *Polym. Degrad. Stab.* **2009**, *94*, 1632–1638.
- (17) del Rio, J. C.; Rencoret, J.; Marques, G.; Gutierrez, A.; Ibarra, D.; Santos, J. I.; Jimenez-Barbero, J.; Zhang, L. M.; Martinez, A. T. Highly acylated (acetylated and/or *p*-coumaroylated) native lignins from diverse herbaceous plants. *J. Agric. Food. Chem.* **2008**, *56*, 9525–9534.
- (18) Martinez, A. T.; Rencoret, J.; Marques, G.; Gutierrez, A.; Ibarra, D.; Jimenez-Barbero, J.; del Rio, J. C. Monolignol acylation and lignin structure in some nonwoody plants: A 2D NMR study. *Phytochemistry* **2008**, *69*, 2831–2843.
- (19) Grabber, J. H.; Mertens, D. R.; Kim, H.; Funk, C.; Lu, F. C.; Ralph, J. Cell wall fermentation kinetics are impacted more by lignin content and ferulate cross-linking than by lignin composition. *J. Sci. Food Agric.* **2009**, *89*, 122–129.
- (20) Yan, J. H.; Hu, Z. J.; Pu, Y. Q.; Brummer, E. C.; Ragauskas, A. J. Chemical compositions of four switchgrass populations. *Biomass Bioenergy* **2010**, *34*, 48–53.
- (21) Samuel, R.; Pu, Y. Q.; Raman, B.; Ragauskas, A. J. Structural characterization and comparison of switchgrass ball-milled lignin before and after dilute acid pretreatment. *Appl. Biochem. Biotechnol.* **2010**, *162*, 62–74.
- (22) Chevanan, N.; Womac, A. R.; Bitra, V. S. P.; Igethinathane, C.; Yang, Y. T.; Miu, P. I.; Sokhansanj, S. Bulk density and compaction behavior of knife mill chopped switchgrass, wheatstraw, and corn stover. *Bioresour. Technol.* **2010**, *101*, 207–214.
- (23) Sluiter, A.; Hames, B. R.; Ruiz, R.; Scarlata, C.; Sluiter, J.; Templeton, D.; Crocker, D. Determination of structural carbohydrates and lignin in biomass. NREL/TP-510-42618, 2010.
- (24) Sluiter, A.; Hames, B. R.; Ruiz, R.; Scarlata, C.; Sluiter, J.; Templeton, D. Determination of ash in biomass. NREL/TP-510-42622, 2008.
- (25) Chum, H. L.; Johnson, D. K.; Black, S. K. Organosolv pretreatment for enzymatic-hydrolysis of poplars 2 - Catalyst effects and the combined severity parameter. *Ind. Eng. Chem. Res.* **1990**, *29*, 156–162.
- (26) Overend, R. P.; Chornet, E. Fractionation of lignocellulosics by steam-aqueous pretreatments. *Philos. Trans. R. Soc., A* **1987**, *321*, 523–536.
- (27) Pedersen, M.; Meyer, A. S. Lignocellulose pretreatment severity—Relating pH to biomatrix opening. *New Biotechnol.* **2010**, *27*, 739–750.
- (28) Boerjan, W.; Ralph, J.; Baucher, M. Lignin biosynthesis. *Ann. Rev. Plant Biol.* **2003**, *54*, 519–546.
- (29) Mueller-Harvey, I.; Hartley, R. D.; Harris, P. J.; Curzon, E. H. Linkage of *para*-coumaroyl and feruloyl groups to cell-wall polysaccharides of barley straw. *Carbohydr. Res.* **1986**, *148*, 71–85.
- (30) Bunzel, M.; Ralph, J.; Funk, C.; Steinhart, H. Structural elucidation of new ferulic acid-containing phenolic dimers and trimers isolated from maize bran. *Tetrahedron Lett.* **2005**, *46*, 5845–5850.
- (31) Buranov, A. U.; Mazza, G. Lignin in straw of herbaceous crops. *Ind. Crops Prod.* **2008**, *28*, 237–259.
- (32) Morrison, T. A.; Jung, H. G.; Buxton, D. R.; Hatfield, R. D. Cell-wall composition of maize internodes of varying maturity. *Crop Sci.* **1998**, *38*, 455–460.
- (33) Ibarra, D.; Chavez, M. I.; Rencoret, J.; del Rio, J. C.; Gutierrez, A.; Romero, J.; Camarero, S.; Martinez, M. J.; Jimenez-Barbero, J.; Martinez, A. T. Structural modification of eucalypt pulp lignin in a totally chlorine-free bleaching sequence including a laccase-mediator stage. *Holzforchung* **2007**, *61*, 634–646.
- (34) Ibarra, D.; Chavez, M. I.; Rencoret, J.; Del Rio, J. C.; Gutierrez, A.; Romero, J.; Camarero, S.; Martinez, M. J.; Jimenez-Barbero, J.; Martinez, A. T. Lignin modification during Eucalyptus globulus kraft pulping followed by totally chlorine-free bleaching: A two-dimensional nuclear magnetic resonance, Fourier transform infrared, and pyrolysis-gas chromatography/mass spectrometry study. *J. Agric. Food. Chem.* **2007**, *55*, 3477–3490.
- (35) Balakshin, M. Y.; Capanema, E. A.; Chen, C. L.; Gracz, H. S. Elucidation of the structures of residual and dissolved pine kraft lignins using an HMQC NMR technique. *J. Agric. Food. Chem.* **2003**, *51*, 6116–6127.
- (36) Ralph, S. A.; Ralph, J.; Landucci, L. *NMR Database of Lignin and Cell Wall Model Compounds*; <http://ars.usda.gov/Services/docs.htm?docid=10491>, 2004.
- (37) Gu, Q.; Rong, Z. Q.; Zheng, C.; You, S. L. Desymmetrization of cyclohexadienones via Bronsted acid-catalyzed enantioselective oxo-Michael reaction. *J. Am. Chem. Soc.* **2010**, *132*, 4056–4057.
- (38) Hong, Y. M.; Shen, Z. L.; Hu, X. Q.; Mo, W. M.; He, X. F.; Hu, B. X.; Sun, N. Acid-catalyzed intramolecular oxa-Michael addition reactions under solvent-free and microwave irradiation conditions. *Arkivoc* **2009**, 146–155.
- (39) El Hage, R.; Brosse, N.; Sannigrahi, P.; Ragauskas, A. Effects of process severity on the chemical structure of *Miscanthus* ethanol organosolv lignin. *Polym. Degrad. Stab.* **2010**, *95*, 997–1003.
- (40) Rencoret, J.; Marques, G.; Gutierrez, A.; Nieto, L.; Santos, J. I.; Jimenez-Barbero, J.; Martinez, A. T.; del Rio, J. C. HSQC-NMR analysis of lignin in woody (*Eucalyptus globulus* and *Picea abies*) and non-woody (*Agave sisalana*) ball-milled plant materials at the gel state 10(th) EWLP, Stockholm, Sweden, August 25–28, 2008. *Holzforchung* **2009**, *63*, 691–698.
- (41) Balakshin, M. Y.; Capanema, E. A.; Chang, H. M. MWL fraction with a high concentration of lignin-carbohydrate linkages: Isolation and 2D NMR spectroscopic analysis. *Holzforchung* **2007**, *61*, 1–7.
- (42) Fasching, M.; Schroder, P.; Wollboldt, R. P.; Weber, H. K.; Sixta, H. A new and facile method for isolation of lignin from wood based on complete wood dissolution. *Holzforchung* **2008**, *62*, 15–23.
- (43) Capanema, E. A.; Balakshin, M. Y.; Chen, C. L.; Gratzl, J. S.; Gracz, H. Structural analysis of residual and technical lignins by H-1-C-13 correlation 2D NMR-spectroscopy. *Holzforchung* **2001**, *55*, 302–308.